Cerebral Cortex September 2009;19:2114–2130
doi:10.1093/cercor/bhn236
Advance Access publication January 15, 2009

Resection of the Medial Temporal Lobe Disconnects the Rostral Superior Temporal Gyrus from Some of its Projection Targets in the Frontal Lobe and Thalamus

Monica Muñoz, Mortimer Mishkin and Richard C. Saunders

Laboratory of Neuropsychology, National Institute of Mental Health, NIH, Building 49, Room 1B80, 49 Convent Drive, Bethesda, MD 20892-4415, USA

Auditory memory in the monkey does not appear to extend beyond the limits of working memory. It is therefore surprising that this ability is impaired by medial temporal lobe (MTL) resections, because such lesions spare working memory in other sensory modalities. To determine whether MTL ablations might have caused the auditory deficit through inadvertent transection of superior temporal gyrus (STG) projections to its downstream targets, and, if so, which targets might have been compromised, we injected anterograde tracer (biotinylated dextran amine) in the STG of both the normal and MTL-lesioned hemispheres of split-brain monkeys. Interhemispheric comparison of label failed to show any effect of the MTL ablation on efferents from caudal STG, which projects to the inferior prefrontal convexity. However, the ablation did consistently interrupt the normally dense projections from rostral STG to both the ventral medial prefrontal cortex and medial thalamic nuclei. The findings support the possibility that the auditory working memory deficit after MTL ablation is due to transection of downstream auditory projections, and indicate that the candidate structures for mediating auditory working memory are the ventral medial prefrontal cortical areas, the medial thalamus, or both.

Keywords: auditory cortex, auditory memory, disconnection, frontal cortex, *Macaca mulatta*

Introduction

Bilateral resection of the medial temporal lobe (MTL) in monkeys produces an auditory memory impairment (see Fritz et al. 2005) just as it does in visual and tactile memory (Mishkin 1978; Murray and Mishkin 1983, 1984). Despite this apparent consistency across sensory modalities, the finding in audition is puzzling for several reasons. Unlike the normal monkeys' memory for visual and tactile stimuli, which can persist long-term, their memory for auditory stimuli decays so rapidly that it seems to reflect working memory exclusively, a time-limited ability that in other modalities is unaffected by MTL removals. Furthermore, although lesions limited to the rhinal cortical areas produce memory deficits in vision and touch that are comparable to those found after removal of the entire MTL (Meunier et al. 1993; Murray et al. 1996; Buffalo et al. 1999; Malkova et al. 2001), rhinal lesions have no effect on auditory memory (Fritz et al. 2005). Enlargement of the rhinal lesion to include the posterior parahippocampal cortex and subadjacent hippocampal formation also leaves auditory memory unaffected. In short, auditory memory is impaired after medial temporal damage only when this region is removed in its entirety, and then the full impairment appears at delays of even a few seconds, that is, it does not seem to vary as a function of delay duration.

Because the effect of the complete MTL removal in audition appears to affect auditory working memory specifically, we explored the possibility that this removal had inadvertently invaded the temporal-lobe white matter containing superior temporal/prefrontal and superior temporal/thalamic projections and thereby disconnected the auditory sensory processing stream from its targets in the frontal lobe and/or thalamus, regions that could well be critical for auditory working memory. Several different lines of evidence support this possibility. First, an impairment qualitatively and quantitatively similar to the one produced by the MTL removal was found after bilateral ablation of approximately the rostral third of the superior temporal gyrus (rSTG, Fritz et al. 2005). Second, prefrontal lesions in the monkey are known to impair performance on a variety of auditory discrimination learning tasks (e.g., Iversen and Mishkin 1973; Lawicka et al. 1975). Third, it has already been shown that aspiration lesions of the MTL interrupt projections to both the prefrontal cortex and medial dorsal nucleus of the thalamus from visual area TE of the inferior temporal gyrus (Baxter et al. 1998; Goulet et al. 1998).

The present study tested whether MTL ablations might similarly interrupt prefrontal and medial thalamic projections known to arise from rSTG (rSTG to prefrontal: Petrides and Pandya 1988; Pandya et al. 1994; Carmichael and Price 1995b; Barbas et al. 1999; Hackett et al. 1999; Kondo et al. 2003. rSTG to medial thalamus: Russchen et al. 1987; Gower 1989; Pandya et al. 1994) and so possibly account for the impairment in auditory memory. To provide an appropriate test, the injected area had to include the entire rSTG, inasmuch as it was damage to this entire area that led to the impairment in auditory working memory, and it is not yet known whether, and if so where, a smaller lesion within the rSTG might reproduce that effect. In addition to testing for the possible transection of rSTG fibers, we also tested an alternative possibility, namely, that MTL ablations might disconnect the inferior prefrontal convexity, an area important for visual working memory (Fuster and Alexander 1971; Goldman-Rakic 1987) from its known inputs originating in more caudal parts of the STG, particularly the belt and parabelt areas (Hackett et al. 1999; Romanski, Bates, et al. 1999).

Materials and Methods

Subjects

Six rhesus monkeys (*Macaca mulatta*) of both sexes weighing between 6.0 and 10.0 kg were used in this study. Experiments were carried out in accord with the Guide for the Care and Use of Laboratory Animals (ILAR, NRC 1996) and under an approved NIMH Animal Study Proposal.

Experimental Plan

Four of the 6 monkeys were prepared with complete forebrain commissurotomy combined with unilateral aspiration of the MTL, after which they received multiple tracer injections into bilaterally symmetrical areas of STG. This design allowed us to identify the locus and extent of a potential disconnection by comparing, within individual animals, the densities of labeled fibers and terminals in a normal hemisphere with those in a hemisphere with the lesion.

Three of the 4 commissurotomized animals (M1–3) received multiple anterograde tracer injections throughout rSTG; these injections covered approximately the rostral third of the gyrus, including the lower bank of the lateral sulcus and the upper bank of the superior temporal sulcus (Fig. 1*a*). The fourth commissurotomized animal (M4)

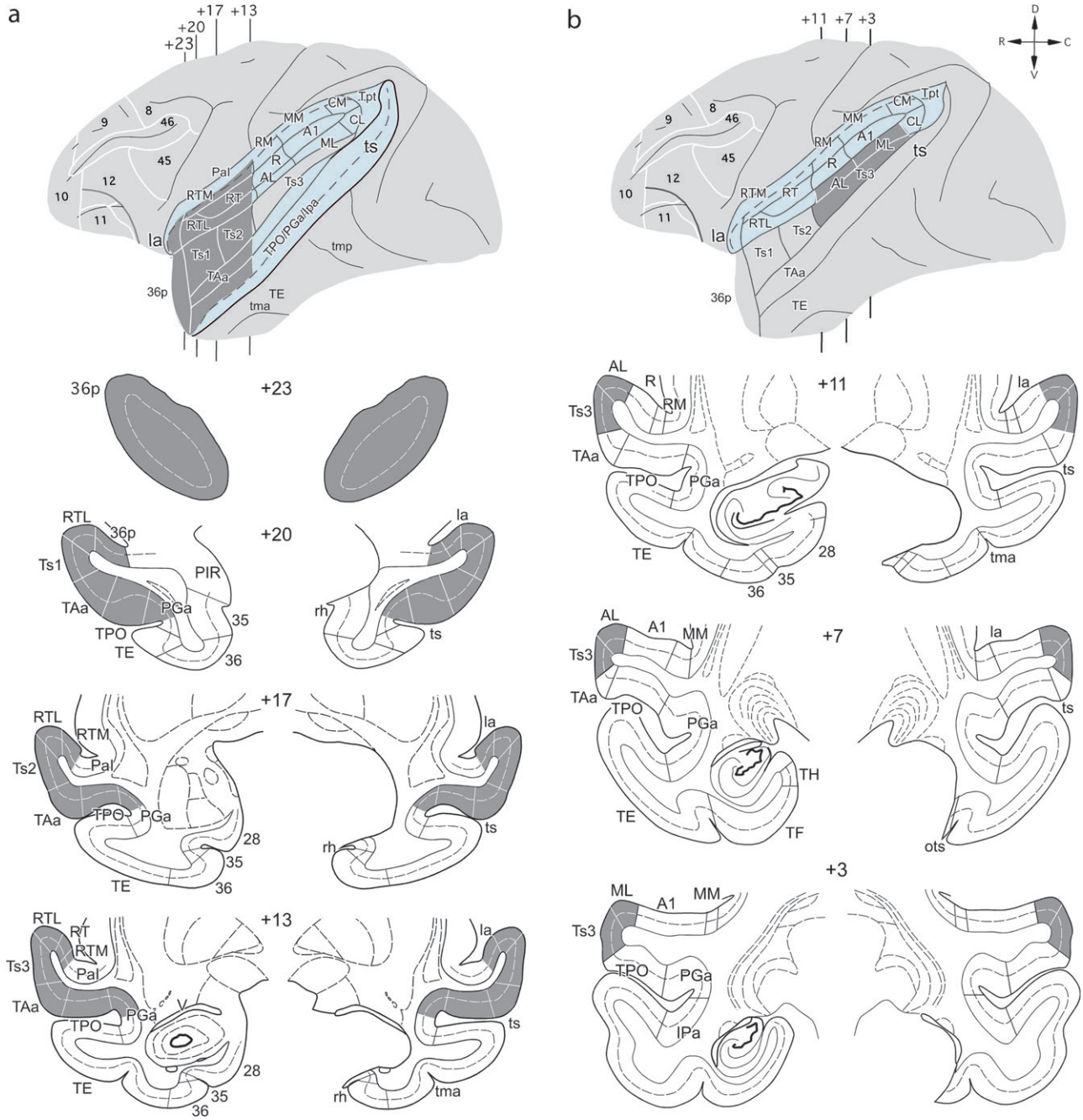

Figure 1. Intended extent of anterograde tracer injections (dark gray areas) in the STG of the rhesus monkey, illustrated on lateral views of the left hemisphere and on coronal sections that also depict a unilateral MTL removal on the right hemisphere. (*a*) Intended injections in rSTG, with "opened" lateral and superior temporal sulci shown in blue. (*b*) Intended injections in caudal STG shown with "opened" lateral sulcus in blue. Numerals preceded by + refer to approximate coronal levels anterior to the interaural plane. la, lateral sulcus; lpa, superior temporal cortical area lpa; ots, occipitotemporal sulcus; Pal, insula, parainsular division; rh, rhinal sulcus; PIR, piriform cortex; RM, rostral medial auditory belt area; tma, anterior middle temporal sulcus; tmp, posterior medial temporal suclus; TF, medial temporal cortical area TF; TH, medial temporal cortical area TH; Tpt, temporoparietal area; ts, superior temporal sulcus; 6, 8, 9, 10, 11, 12, 13, 14, 24, 25, 28, 32, 35, 36, 45, 46, Brodmann's cytoarchitectonic areas; 36p, temporal pole division of Brodman's area 36; A1, auditory core area A1; AL, anterior lateral auditory belt area; ML, middle lateral auditory belt area; MM, middle medial auditory belt area; PGa, superior temporal gyrus area; PGa, R, auditory core area R; RT, auditory core area RT; RTL, rostrotemporal lateral auditory belt area, RTM; rostrotemporal medial auditory belt area; TAa, superior temporal gyrus area TAa; TE, inferior temporal gyrus area TE; TPO, superior temporal gyrus area TPO; Ts1, superior temporal gyrus area Ts1; Ts2, superior temporal gyrus area Ts2; Ts3 superior temporal gyrus area Ts3; V, temporal horn of the lateral ventricle.

received multiple anterograde tracer injections in the lateral belt and parabelt auditory regions and the laterally adjacent part of Ts3 of caudal STG (Fig. 1*b*).

The 2 additional monkeys (M5–6) received unilateral anterograde tracer injections into rSTG; one of these (M5) was an animal with a bilateral MTL ablation from the impaired group in the auditory memory study (Fritz et al. 2005), and the other (M6) was an unoperated control. The rSTG area receiving tracers in these 2 animals was the same as that in cases M1–3, except that the lower bank of the lateral sulcus was excluded in order to avoid injecting tracers into the subjacent white matter (see Results).

Surgical and Injection Procedures

For each surgery, the animal was initially sedated with Ketamine (Ketamine HCl, 10 mg/kg), intubated, and then maintained at a surgical level of anesthesia with isoflurane (1–4%, to effect). The animal was wrapped in a heating blanket with its head secured in a head holder, its vital signs (heart rate, respiration rate, temperature, oxygen saturation, and CO_2) monitored continually, and intravenous fluids provided throughout. For the commissurotomy, unilateral bone and dural flaps were turned to expose the cerebral midline, and, with the aid of an operating microscope, the corpus callosum and anterior commissure were visualized and then transected using a small glass pipette. The dural flap was then replaced, the bone flap sewn in position, and the wound closed in anatomical layers. A prophylactic dose of antibiotics and analgesics was administered, and this treatment was continued postoperatively as warranted.

For the unilateral ablation of MTL, frontotemporal bone, and dural flaps were turned and, again with the aid of the operating microscope, the tissue medial to the rhinal and occipitotemporal sulci was aspirated using a small-gauge metal suction tube. The unilateral removal, which was on the left in all cases except in M3 and M4, included the amygdala and the perimaygdaloid cortex, entorhinal cortex, the hippocampus proper, subiculum, presubiculum, and parasubiculum, as well as the posterior parahippocampal cortex. This is the same lesion that had been performed bilaterally in animals that showed subsequent auditory memory impairment (Fritz et al. 2005). The commissurotomy and unilateral medial temporal ablation were performed in 2 stages, in that order, separated by at least one month, except in M3, which received both surgical procedures in one stage.

The cranial opening for the MTL removal also provided access to 1) the rSTG, in which 20–25 1-μL injections of the anterograde tracer biotinylated dextran amine (BDA 10K MW, 10% BDA in 0.01 M phosphate buffer, Molecular Probes, Inc., Eugene, OR) were made every 2 mm in a grid-like fashion along the rostral 15–17 mm of STG in all cases except M4 (Fig. 1*a*); and 2) caudal STG, in which nine 1-μL BDA injections were placed along the lateral belt and parabelt region of the auditory cortex in case M4 (Fig. 1*b*). Once the injections were completed the dura was sutured, the bone flap replaced, and the wound closed in anatomical layers. Prophylactic doses of antibiotics and analgesics were administered as before.

Perfusion and Tissue Processing

Fourteen days after receiving BDA injections the animals were deeply anesthetized with pentobarbital and transcardially perfused with 500 cm^3 of saline, followed by 500 cm^3 of 1% paraformaldehyde and 8 L of 4% paraformaldehyde, both in 0.1 M phosphate buffer (pH 7.4) at room temperature. Brains were removed from the skull, photographed, blocked in the coronal plane, and then cryoprotected through a series of glycerols (Rosene et al. 1986). Brains were quickly frozen in –80 °C isopentane and stored until they were sectioned, at which time they were cut in the coronal plane at 50 μm. For the brains with the BDA injections, 2 adjacent 1-in-10 series were processed, one treated to visualize BDA (see below) and the other stained with thionin. The thionin series was used to identify cytoarchitectonic borders.

The BDA series was stained using an avidin–biotin horseradish peroxidase technique (Reiner and Gamlin 1980; Veenman et al. 1992). Endogenous peroxide was inhibited by a 30-min wash in 1% hydrogen peroxide. The tissue was then incubated for 4 h at room temperature and overnight at 4°C with a concentration of 0.5 μg/mL of avidin horseradish peroxidase or streptavidin horseradish peroxidase conjugate (Molecular Probes, Inc., Eugene, OR) in 0.05 M Tris buffer (pH 7.6). The chromogen reaction was conducted with 3,3-diaminobenzidine tetra hydrochloride reaction (DAB, Sigma Co, St Louis, MO) at a concentration of 0.05% with 0.03% hydrogen peroxide and 0.1–0.2% nickel sulfate in 0.05 M tris buffer (pH 8.0) to intensify the staining. The reaction was monitored with a microscope and stopped after 3–5 min to maximize fiber staining while minimizing background. Sections were then mounted, dehydrated, and coverslipped.

Analysis

All brains were examined using a Zeiss microscope equipped with a digital video camera (CCD, Optronics, Goleta, CA) and an image analysis system (Bioquant Nova, R&M Biometrics, Inc., Nashville, TN). The area of effective uptake of the BDA tracer was defined on each section as the area in which the cortical laminar pattern was obscured by the anterograde-tracer label (Figs 2, 3) and expressed as a percentage of the intended area of injection. Detailed anatomical drawings of the BDA-labeled fibers and terminal fields in the frontal cortex and thalamus were traced from the coronal sections using an Aus Jena projector (6.5×). The cytoarchitectonic borders were determined from microscopic examination of the adjacent thionine-stained sections.

Nomenclature

Superior Temporal Gyrus

As delineated in Figure 1, rSTG covers the rostral 15–17 mm of the STG. This rostral region includes 1) the cytoarchitectonic subdivisions 36pm and 36pl of the temporal pole, as described by Insausti et al. (1987); 2) the cytoarchitectonic areas Ts1, Ts2, Ts3 (superior temporal cortical areas Ts1, Ts2, Ts3), superior temporal cortical area TPO, superior temporal cortical area PGa, and superior temporal cortical area TAa (rostral part), as defined by Pandya and his colleagues (Pandya and Sanides 1973; Seltzer and Pandya 1978, 1989b); and 3) the cytoarchitectonic areas rostrotemporal lateral auditory belt area (RTL), auditory core area RT (RT), and rostrotemporal medial auditory belt area (RTM), as defined by Kaas and Hackett (2000) for the rostral portion of the supratemporal plane (STP), which lie in the ventral bank of the lateral sulcus and differs cytoarchitectonically from areas Ts1–3 on the adjacent lateral convexity of rSTG. The remaining auditory core and belt areas (i.e., A1/R [auditory core area A1/auditory core area R], AL [anterior lateral auditory belt area], ML [middle lateral auditory belt area], middle medial auditory belt area, caudolateral auditory belt area, and CM [caudomedial auditory belt area]), located caudally in the STP, were delineated according to Kass and Hackett (2000).

Frontal Cortex

The cytoarchitectonic divisions of the frontal cortex were adapted from the descriptions in *Macaca mulatta* originally given by Walker (1940) and revised later by Pandya and his colleagues (Barbas and Pandya 1989; Pandya and Yeterian 1990; Petrides and Pandya 1999, 2002) and Carmichael and Price (1994).

Thalamus

The thalamic nuclei were delineated in accordance with Olszewski (1952).

Results

Forebrain Commissurotomy and MTL Ablation

The transections of the corpus callosum and anterior commissure were complete in each case, and there was no evidence of damage to adjacent structures (Fig. 2). Also as intended, the MTL removal in each case included the amygdala and perimaygdaloid cortex, entorhinal cortex, hippocampus

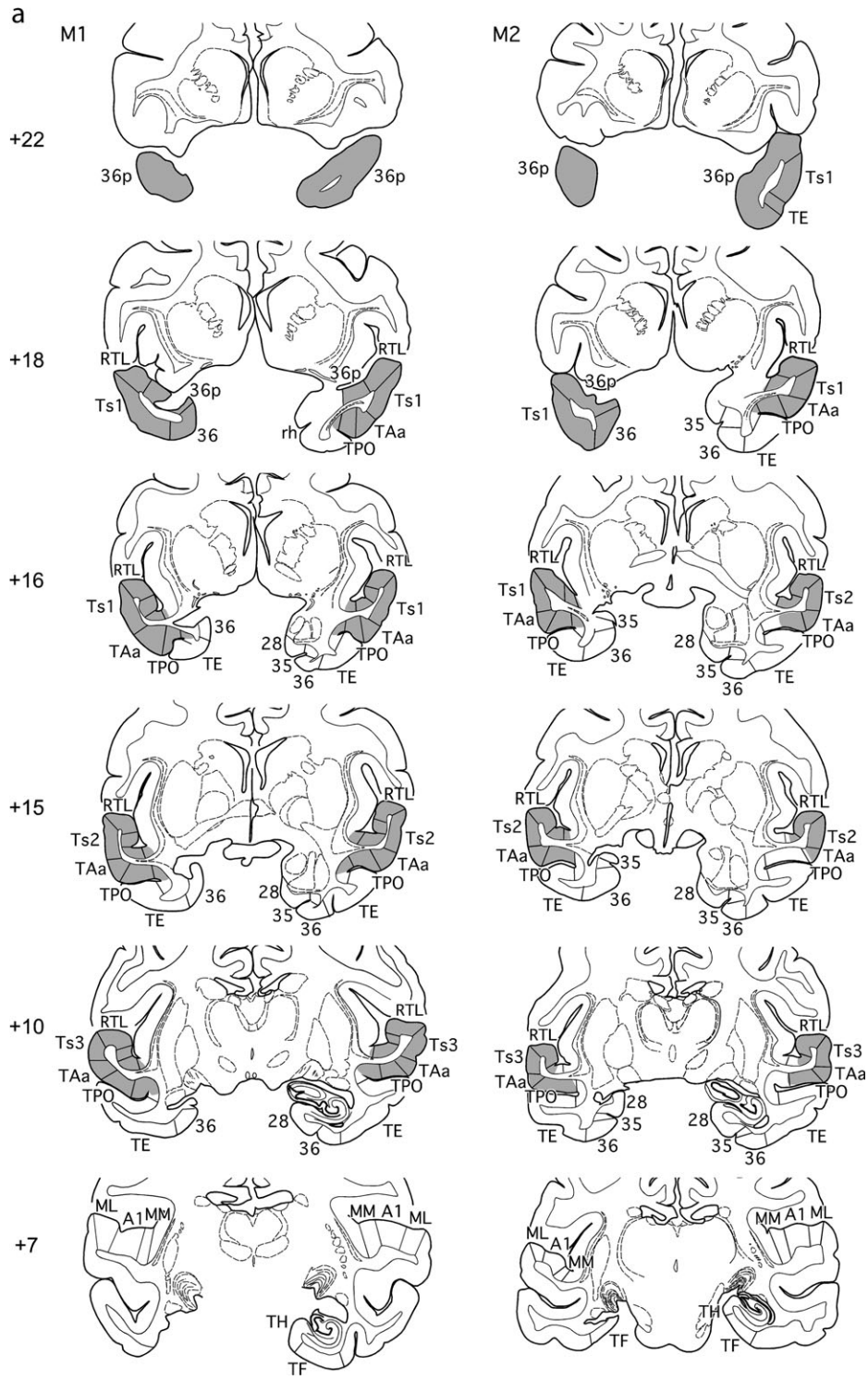

Figure 2. (*a*, *b*) Series of rostral (top) to caudal (bottom) coronal sections from cases M1 and M2 (*A*) and from cases M3 and M4 (*b*) illustrating the extents of the bilateral tracer injections in gray, as well as the unilateral MTL removals and forebrain commissurotomies. Note that the MTL removal was on the left in cases M1 and M2 and on the right in the others. Numerals preceded by + refer to approximate coronal levels anterior to the interaural plane. See Figure 1 for abbreviations.

proper, subiculum, presubiculum, and parasubiculum, as well as posterior parahippocampal cortex. However, cases M4 and M5 sustained unintended bilateral damage to the tail of the caudate nucleus and ventral portion of the putamen. As noted earlier, case M5 was the animal with a bilateral MTL ablation from the impaired group in the auditory memory study, although other equally impaired animals in that group did not sustain this inadvertent damage (Fritz et al. 2005).

Tracer Injections

The bilateral injections were highly symmetrical in all animals. They covered approximately 90 percent of the intended target

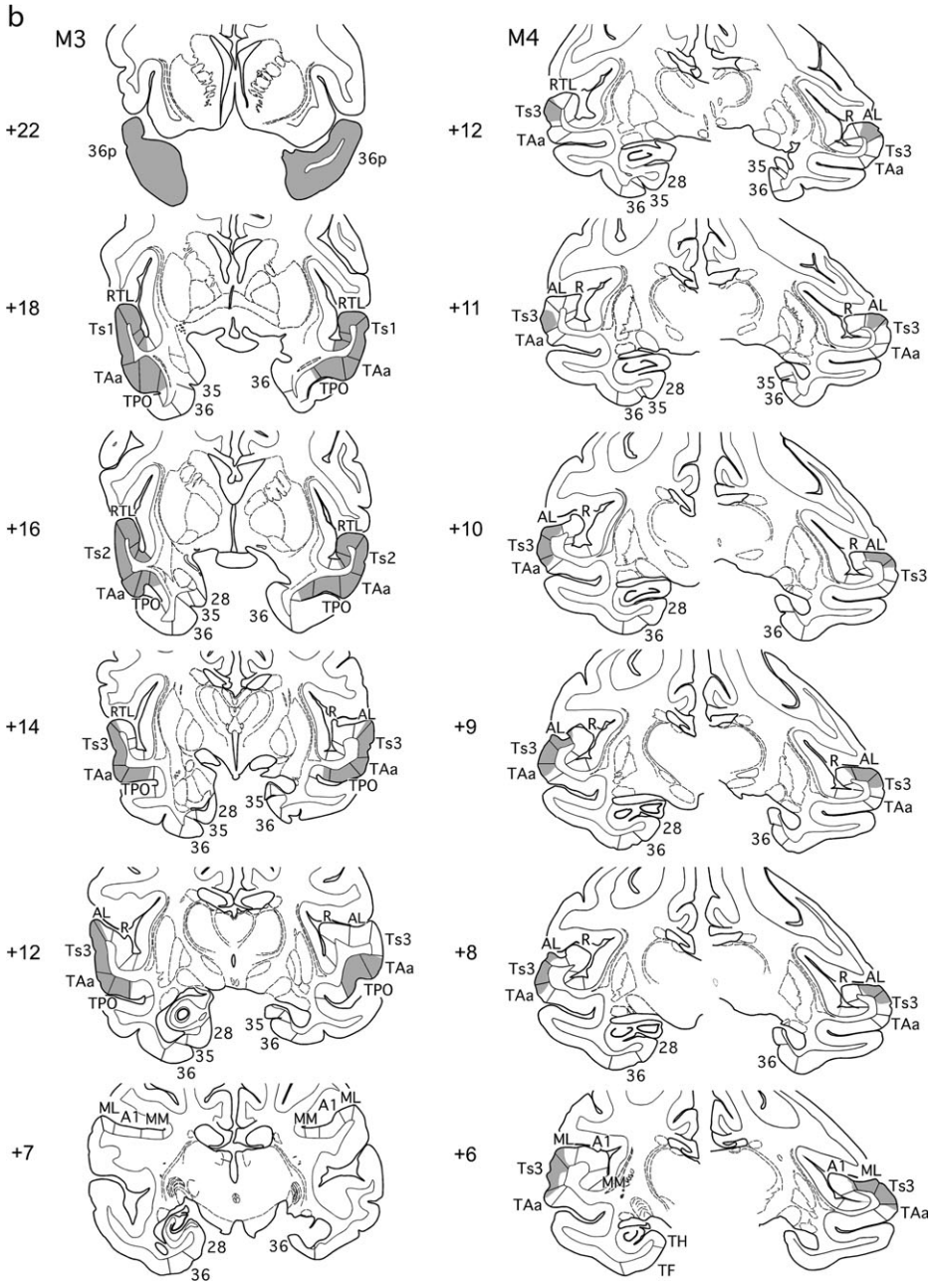

Figure 2. (Continued).

area in both the normal and MTL-lesioned hemispheres in cases M1-M3 (Figs 2 and 3).

Because the BDA injections in the lower bank of the lateral sulcus in cases M1–3 encroached on white matter in the dorsal part of rSTG, fibers of passage from posterior portions of STG could have been transected, and consequently these transected fibers could have taken up and transported the tracer. To avoid this potential problem in cases M5 and M6, we omitted the lateral sulcal injections in these 2 animals and therefore covered only about 60% of the area targeted in cases M1–3. Careful comparison of the results after the 2 types of injections failed to reveal a clear and consistent difference in the pattern or density of projections to the frontal lobe and diencephalon in either the normal or MTL-lesioned hemispheres. This negative finding is consistent with the results of Saleem et al. (2008), who showed after a series of retrograde tracers in the ventral medial frontal cortex that the majority of such projections originate from the gyral surface and upper bank of the superior temporal sulcus. It is therefore unlikely that possible invasion of white matter in cases M1–3 affects the interpretation of the results reported here. Furthermore, the frontal projection pattern after the caudal STG injections in case M4 (see also Petrides and Pandya 1988; Hackett et al. 1999; Romanski, Bates, et al. 1999; Romanski, Tian, et al. 1999; Saleem et al. 2008) overlapped little if at all with that found after the rSTG injections, again rendering unlikely any misattribution of the results in the first 3 animals.

The BDA injections in caudal STG of case M4 covered more than 90% of the auditory lateral belt areas AL and ML in the

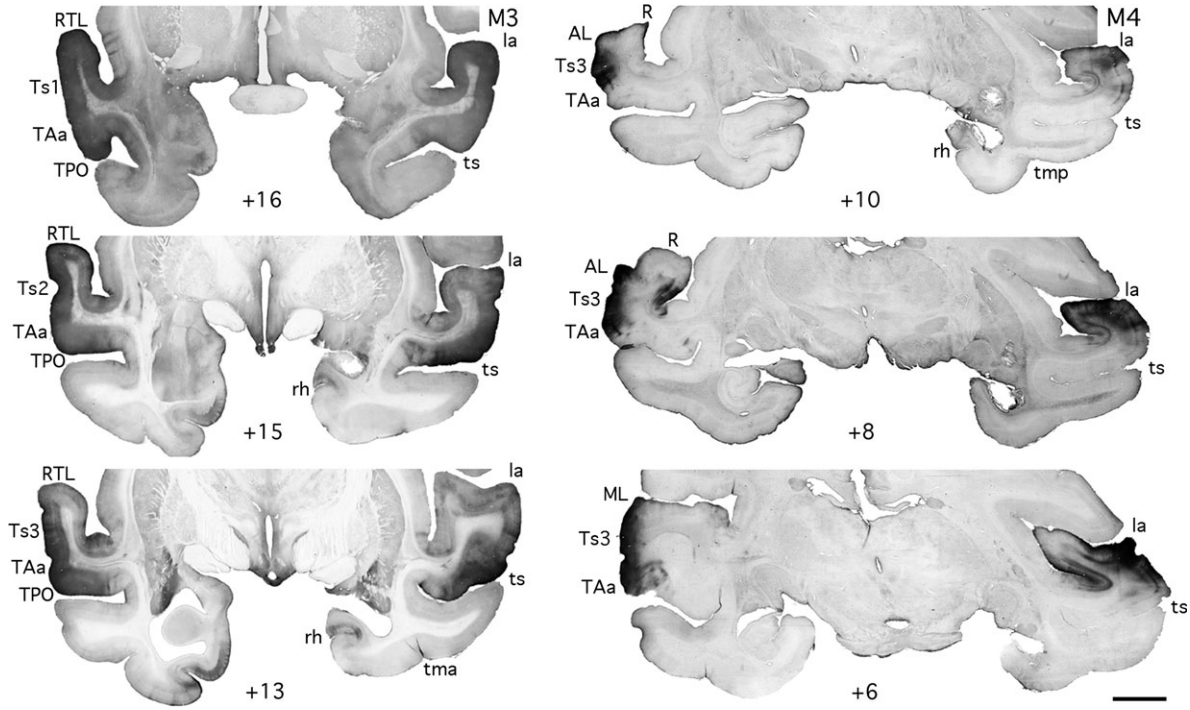

Figure 3. Photomicrographs of coronal sections illustrating the actual BDA injection areas in rostral (case M3) and caudal (case M4) STG. Scale bar: 1.4 cm. See Figure 1 for abbreviations.

MTL-lesioned hemisphere and about 80% in the normal one. These injections also included the most lateral aspect of the core auditory areas A1/R and the caudal end of areas RTL and Ts3 (Figs 2 and 3).

The effect of the forebrain commissurotomy on the efferent projections of rSTG was assessed by comparing the results in cases M1–3 with those in cases M5 and M6, which had no commissurotomy. There was no noticeable difference in pattern or density of BDA label between the injected hemisphere of M5 and the operated hemispheres of M1–3, or between the injected hemisphere of M6 and the unoperated hemispheres of M1–3. There was also no detectable difference in pattern or density of label related to side of the unilateral MTL removal, which was performed in the left hemisphere in cases M1–2 and in the right in case M3.

Anterograde Label after Injections in rSTG: Normal Hemispheres

The following descriptions of label in the frontal lobe and thalamus refer specifically to that found in the normal right hemisphere of case M2 (Fig. 4) and M3 (Fig. 5), respectively, but they also apply as well to the normal hemispheres of the other cases.

Frontal Lobe

The densest anterograde label outside the temporal lobe was found in the frontal lobe. The entire frontal cortical label appeared to originate from fibers leaving the rSTG to form part of the uncinate fasciculus (UF) and extreme/external capsules. Fibers arising from the temporal pole coursed caudally in the white matter and converged at the frontotemporal junction with fibers originating in areas Ts1-Ts3, TPO, and RTL. Fibers that coursed in the UF (in Fig. 4*h*) had a funnel-like appearance at the frontotemporal junction as they ascended dorsally towards the frontal lobe (Fig. 4*e–h*). Other labeled fibers coursed in the white matter of the STG and crossed the extreme capsule, claustrum, and external capsule adjacent to the ventral lateral perimeter of the putamen (Fig. 4*i-l*), and emerged in the frontal lobe, where they converged with the fibers from the UF (Fig. 4*a–g*). This dense pathway of labeled fibers coursed through the white matter beneath the medial frontal and orbitofrontal cortical areas (Fig. 4*a–g*) with the highest density terminating in the ventral medial frontal and orbitofrontal cortical areas.

In the medial frontal cortex (Fig. 4*a-g*), labeled fibers emerged from the white matter within the gyrus rectus with dense terminal label in areas 14, 25, 32, and 24. There was much lighter label in areas 9 and 10. In all areas the fibers coursed through the deep layers terminating primarily in layers I–III. The label in areas 24 and 32 had a patchier appearance than that in area 25, with an occasional columnar-like arrangement. Also, the terminal label in area 24 was not uniform along its rostrocaudal extent; the highest density was located rostral to the genu of the corpus callosum (Fig. 4*d*), whereas only sparse label was found caudal to the genu (Fig. 4*g*). The pregenual terminations arose from the labeled fibers in the white matter deep to gyrus rectus and area 32, whereas the postgenual terminations appeared to arise from labeled fibers that coursed through the extreme capsule, pierced the claustrum, passed through the external capsule, and then continued lateral and dorsal to the head of the caudate nucleus towards area 24 (Fig. 4*e,f*). A moderate to light density of labeled axons continued dorsal to the cingulate sulcus to end in layers I–III of the medial portion of area 9 (Fig. 4*b,c*).

In the orbital frontal cortex, labeled fibers emerged in an arch-like pattern from the white matter deep to the fundus of the medial orbital sulcus (Fig. 4*a-g*). This label, which was

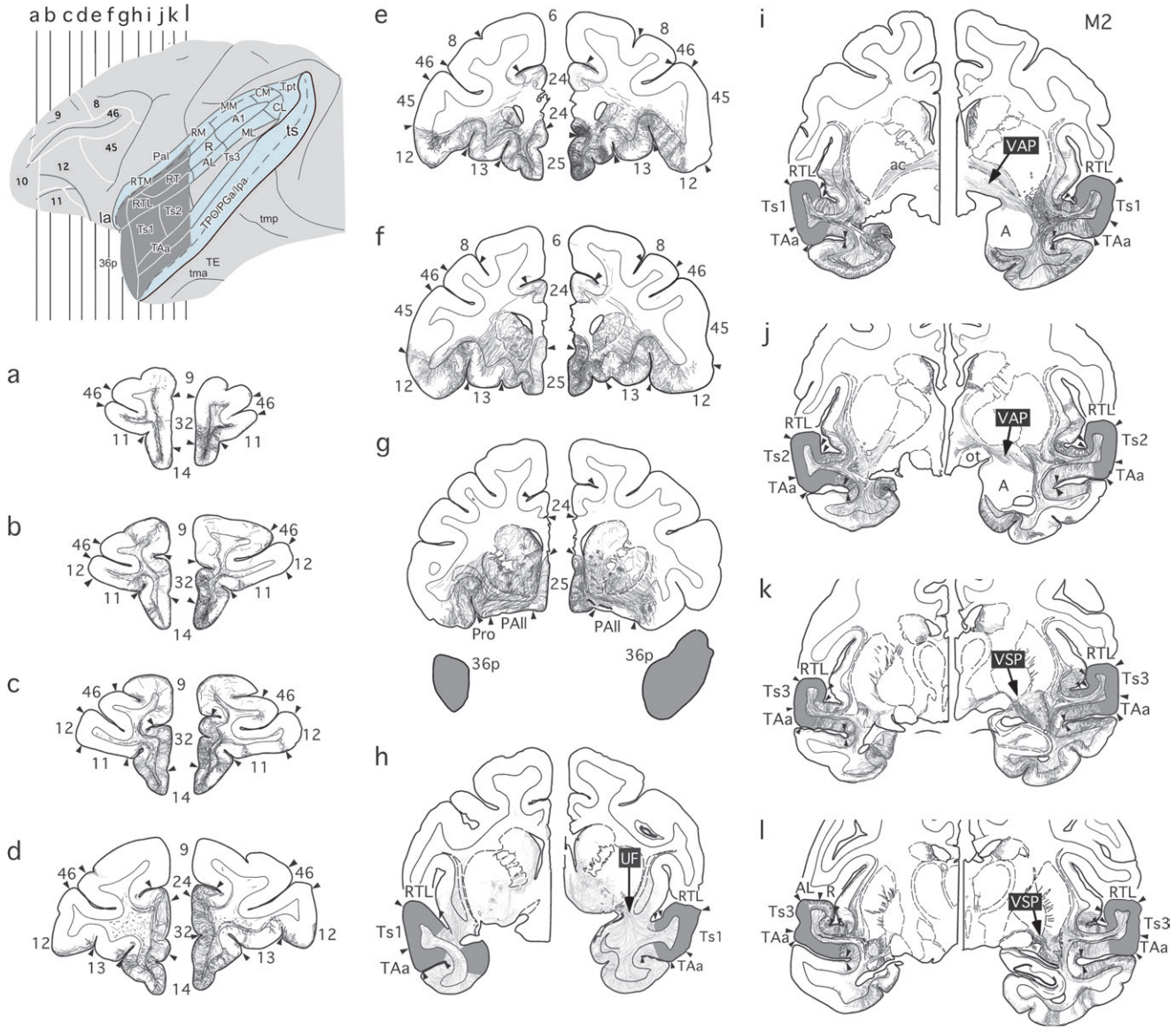

Figure 4. Lateral surface view and coronal sections (*a–l*) illustrating anterograde tracer injections (dark gray) in rSTG, with "opened" lateral and superior temporal sulci shown in blue, and resulting fiber and terminal label in case M2. In the intact right hemisphere, labeled efferent fibers from the injected STG region joined 3 major pathways: One coursed through the uncinate fasciculus (*h*) and led to dense terminal label in the ventral medial frontal cortex (*a-g*), whereas a second and third followed the ventral amygdalofugal (*i*, *j*) and ventral striatum pathways (*k*, *l*), leading to dense terminal label in the medial thalamus. In the hemisphere with the MTL removal, all 3 efferent pathways were interrupted resulting in substantially less dense label in these 2 target areas. A, amygdala; 13, 14, 24, 25, 32 Brodman's cytoarchitectonic areas; ai, inferior arcuate sulcus; as, superior arcuate sulcus; p, principal sulcus; PAll, frontal periallocortical area; Pro, proisocortex; UF, uncinate fasciculus; VAP, ventral amygdalofugal pathway; VSP, ventral striatum pathway; see Figure 1 for abbreviations.

much less dense than that in the medial frontal areas, could be observed along the entire rostrocaudal extent of the medial orbital sulcus, with fibers terminating primarily in layers V–VI and I–III of area 14. In addition, labeled fibers from this bundle passed laterally in the white matter deep to the lateral orbital sulcus with fibers emerging to terminate primarily in layers V–VI and I–III of areas 13 and caudal 12, in Pro (proisocortex) and PAII (frontal periallocortical area), and as far forward as area 11. The densest terminal label from this fiber bundle was found in the caudal part of area 13 and the caudomedial part of area 12, particularly in the banks and depths of the lateral orbital sulcus (Fig. 4*e-f*), with occasional columnar-like arrangement of labeled fibers in this region (e.g., Fig. 4*e*).

In the lateral prefrontal areas, a very light band of labeled fibers emerged in the white matter deep to the principal sulcus and terminated primarily in layers I–III in the fundus and dorsal bank of the rostral part of the principal sulcal area 46. Only a light density of label was found in the part of area 12 on the lateral surface, and no label was observed in areas 45 or 8.

Thalamus

A second major route taken by labeled fibers from the rSTG coursed immediately lateral and dorsal to the amygdala and pes hippocampus (Fig. 4*k,l*) to form part of the ventral amygdalofugal pathway (VAP, Fig. 4*i,j*), with terminations in the thalamus (Fig. 5, case M3, normal left hemisphere). The rostral portion of this dense band of fibers passed ventral to the anterior commissure (Fig. 4*i*) and targeted the medial diencephalon. At a slightly more caudal level (Fig. 4*j*), fibers traveled between the optic tract and globus pallidus en route to the medial thalamus. Still more

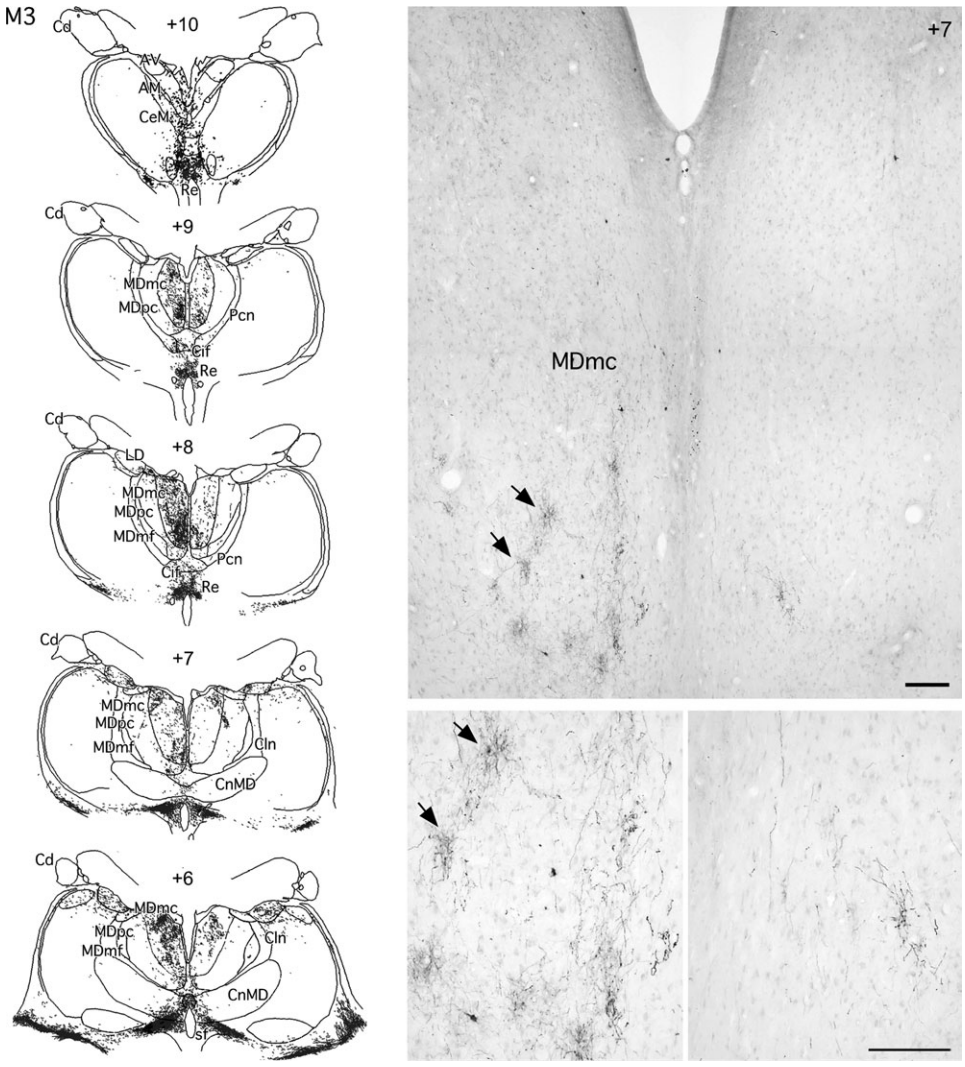

Figure 5. Coronal sections and photomicrographs from case M3 showing the distribution of anterograde label in the medial thalamus after bilateral BDA injections in the rSTG. Photomicrographs at 2 different magnifications illustrate the patchy distribution of the label in the magnocellular portion of the medial dorsal nucleus of the thalamus. Note the decreased density of label in the right hemisphere with the MTL ablation. Scale bar: 250 μm. Cln, central lateral thalamic nucleus; CnMD, centrum medianum thalamic nucleus; Cd, caudate nucleus; Pcn, paracentral nucleus; CeM, central medial thalamic nucleus; AD, anterior dorsal thalamic nucleus; AM, anterior medial thalamic nucleus; AV, anterior ventral thalamic nucleus; Cif, central inferior thalamic nucleus; Cim, central intermedial thalamic nucleus; MDmc, medial dorsal thalamic nucleus magnocellular division; MDmf; medial dorsal thalamic nucleus multiformis division; MDpc, medial dorsal thalamic nucleus parvocellular division; Pcn, paracentral nucleus; Pf, parafascicular nucleus; Re, Reuniens; Ro, Rotundus; sf, subfascicular nucleus.

caudally, a third route of labeled fibers formed part of a ventral striatal pathway (VSP) and passed through the sublenticular and retrolenticular segment of the internal capsule. This bundle of fibers, which passed between the ventral claustrum and ventral perimeter of the putamen, and dorsal to the tail of the caudate nucleus, continued medially between the optic tract and globus pallidus to access its medial thalamic targets (Figs 4*k*,*l* and 5). More caudally still, this dense band coursed dorsal to the lateral geniculate nucleus (LGN), and its trajectory could also be tracked as far as the medial thalamus (Fig. 5).

In the thalamus, light to moderate terminal label was seen in the anterior thalamic nuclei (AV [anterior ventral thalamic nucleus], AM [anterior medial thalamic nucleus], AD [anterior dorsal thalamic nucleus]) and lateral dorsal nucleus (LD), with denser label in the magnocellular division of the medial dorsal nucleus (MDmc), which contained small arborizations of short axons rich in terminals (Fig. 5). By contrast, in other medial dorsal thalamic nucleus (MD) subdivisions (MDpc [parvocellular division of the medial dorsal nucleus] and MDmf [multiformis division of the medial dorsal nucleus]), only light anterograde label was observed. Dense to moderate label could also be seen in some of the midline thalamic nuclei, including centrum inferior (Cif), centrum inferior medianum (Cim), rotundus (ro), subfascicularis (Sf), and reuniens (Re), and also in the medial parts of centrum medianum (CnMd) and the parafascicular nucleus (Pf).

Finally, labeled fibers from the rSTG traveled through the temporo-pulvinar bundle of Arnold located in the sublenticular segment of the internal capsule to terminate heavily in the medial pulvinar (not shown).

Summary of Anterograde Label in Normal Hemispheres

The fibers labeled by the BDA injections in the rSTG took 3 major routes. One route formed part of the UF and the ventral part of the extreme and external capsules. These fibers terminated extensively throughout the ventral medial areas

(areas 25, 14, 32, and 24) of the medial frontal cortex. There was less dense label in the medial part of areas 9 and 10, and caudal orbitofrontal areas Pro, PAII, 13, 12, and caudal 11. A light band of labeled fibers and terminals was observed in dorsolateral areas 46 but no label was seen in the dorsolateral part of area 9 or in areas 45 or 8.

The second major projection comprised labeled fibers leaving the rSTG and coursing immediately lateral and dorsal to the amygdala and then merging with the VAP, whereas a third projection contributed to a VSP. Labeled fibers from these pathways reached the thalamus, where a high density of anterograde label was observed in MDmc and medial pulvinar, and more moderate label in the anterior, lateral dorsal, and midline nuclei.

Anterograde Label after Injections in rSTG: Hemispheres with MTL Lesions

The following description refers specifically to the MTL-lesioned left hemisphere in case M2 shown in Figure 4, but it applies as well to the MTL-lesioned hemispheres in cases M1, M3, and M5.

Frontal Lobe

As in the normal hemispheres, labeled fibers from rSTG in the MTL-lesioned hemispheres converged near the frontotemporal junction comprising part of the UF. At this junction, however, encroachment of the MTL aspiration lesion on white matter just lateral to the piriform cortex and rostral amygdala (constituting the anterior part of the MTL ablation) interrupted the labeled fibers (Figs 4*b-l* and 6, compare *a* with *b* and, at higher magnification, *c* with *d*). As a result, there was a dramatic reduction in the lesioned compared with the normal hemisphere in the density of labeled UF fibers entering the frontal lobe (Fig. 7). A concomitant reduction in terminal label was observed in ventral medial frontal cortical areas 25, 14, and PAII as well as in dorsomedial areas 32 and pregenual 24 (Figs 4*a-g* and 7). This striking decrease in medial frontal cortical label was observed in all hemispheres with the MTL removals. The density of label in areas 10 and 9 was very light in normal hemispheres and there were no noticeable reductions of density in hemispheres with the MTL lesion.

The arch-like bundle of labeled UF fibers found in the white matter of the medial orbital sulcus in the normal hemispheres was also markedly decreased in fiber density in the hemispheres with the MTL ablation, but only in the most medial part of this pathway, which presumably contributed to the substantial decrease in terminal label already noted in ventral medial areas 25, 14, and PAII. By contrast, labeled fibers and terminals from the more lateral part of this pathway, which project to orbitofrontal areas Pro, 13, 12, and 11 (Fig. 4*a-f*) and also to area 46 on the lateral surface, appeared unaffected, with equal density of label in the 2 hemispheres.

Thalamus

The other major route out of rSTG, this one formed by labeled fibers coursing lateral and dorsal to the amygdaloid complex, was also interrupted by the white matter damage accompanying the MTL ablation (Figs 4*i,j* and 6). Consequently, labeled fibers from rSTG that normally merge with the VAP were almost absent in the hemispheres with MTL lesions (Figs 4*j-l* and 6, compare *e* with *f* and *g* with *h*). Fibers forming the route out of rSTG that normally join the VSP to constitute its most rostral aspect were also transected (Figs 4*k,l* and 6*i-l*). The transection of these 2 sets of fibers was accompanied by a clear decrease in density of labeled axons and terminals in the anterior thalamic nuclei (AV, AM, AD), MDmc, and some of the nuclei at the midline (Cif, Cim, Pf, Sf, and the medial portion of CnMd; Fig. 5). Because the density of label in MDpc and MDmf was much lighter than in MDmc, any difference between the lesioned and normal hemispheres would be difficult to detect, and none was seen. The source and route of the fibers terminating in the LD nucleus and the medial pulvinar lay caudal to the MTL ablation (see Saunders et al. 2005), and consequently the labeling was the same in the lesioned and normal hemispheres.

The effects of the MTL lesion on this major rSTG projection pathway was exacerbated in case M5 by the infarcts in the tail of the caudate nucleus, which resulted in damage to fibers that normally course in the VSP, that is, dorsal to both this nucleus and the optic tract, on their way to the medial diencephalon, and therefore interrupting rSTG-diencephalic projections even more severely. However, despite this apparent increase in damage to fibers projecting to the thalamus, we were not able to detect a greater decrease in thalamic terminal label. Except for these infarct-related effects, the caudal part of the MTL removal did not appear to interrupt any of the rSTG projections (e.g., Fig. 6*m,n*).

Anterograde Label after Injections in Caudal STG: Normal Hemisphere

Frontal Lobe

Compared with the medial and orbital frontal lobe label in the cases given BDA injections in rSTG, the frontal lobe of case M4, which received BDA injections in the auditory belt and parabelt areas, contained only low to moderate density of anterograde label (Fig. 8). Labeled axons originating in these caudal areas of the normal hemisphere formed a bundle within the STG white matter that branched to form 2 pathways. One coursed rostrally within the white matter of the STG and appeared to terminate in portions of rSTG, with occasional column-like appearance in both areas RTL and RT, Ts2, and the dorsomedial division of the temporal pole (Fig. 8*d–f*). The second pathway exited the white matter of the STG and passed through the ventral third of the extreme and external capsules. At the level of the LGN, this label occupied only the ventral half of the extreme and external capsules, whereas at the level of the amygdala the label occupied the whole dorsoventral extent of both capsules. As shown in Figure 8, fibers coursed rostrally and crossed the frontotemporal junction just dorsal to the UF (Fig. 8*d,e*) to reach the frontal lobe (Fig. 8*a–c*). The white matter of the inferior frontal gyrus contained most of the labeled fibers of this pathway, some of which turned laterally to reach area 45 and parts of area 46 (Fig. 8*a,b*). A few labeled fibers continued in the white matter deep to area 11 to terminate medially in area 32 and laterally in dorsal portions of areas 46 and adjacent 9 (not shown).

Thalamus

Some of the fibers within the second of the 2 pathways described above continued dorsal to the LGN ending with light label in the medial geniculate nucleus, suprageniculate nucleus, and ventral portion of the posterior pulvinar. No label was

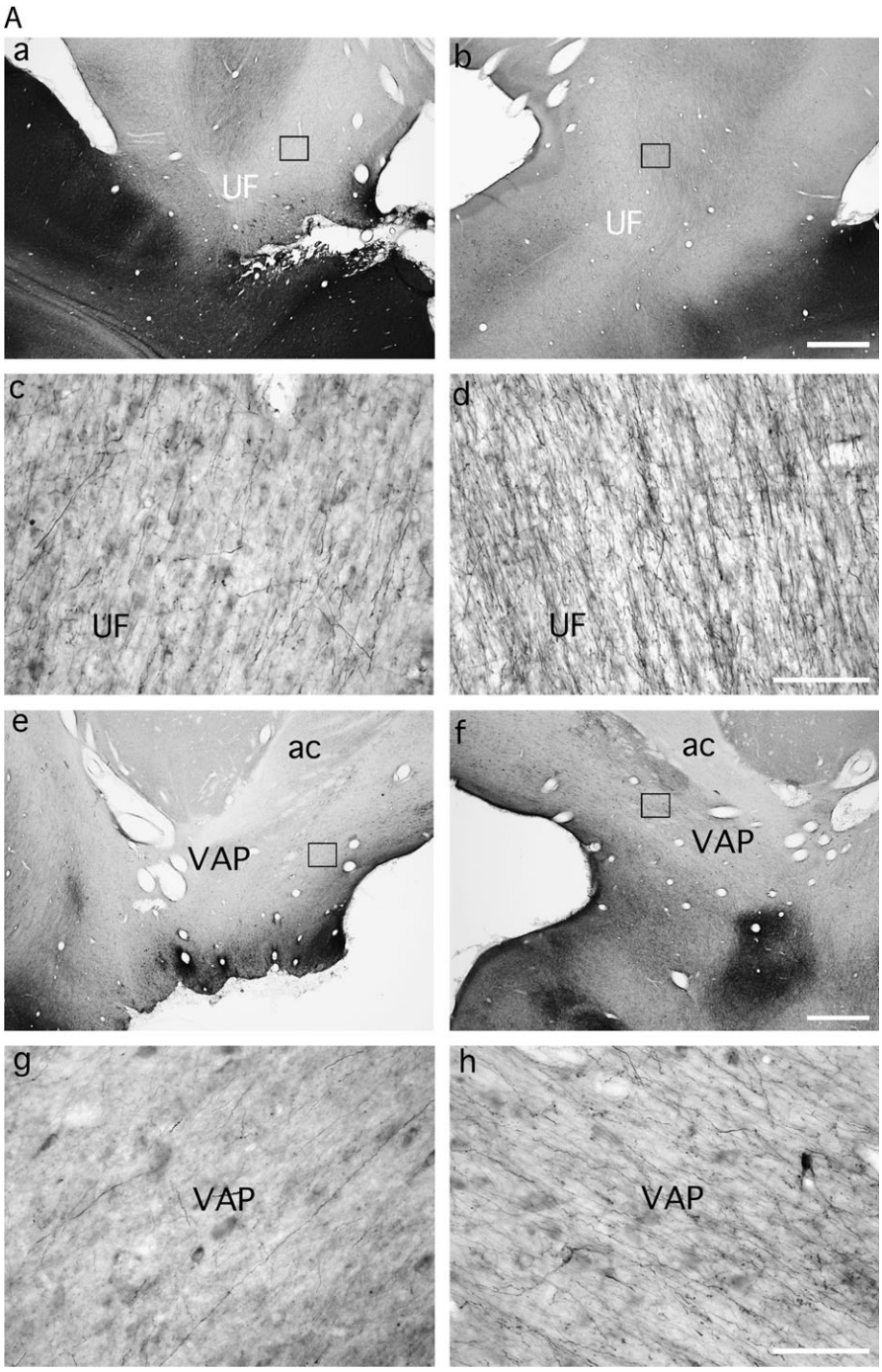

Figure 6. (*a*, *b*) Photomicrographs from case M2 showing the disruption of the labeled fibers in the UF (UF, *a–d*), the VAP (*e–h*), and the VSP (*i–n*), after left MTL removal relative to the normal contralateral hemisphere. Scale bars *a*, *b*, *e*, *f*, *i*, *j*, *m*, *n*: 1 mm; *c*, *d*, *g*, *h*, *k*, *l*: 100 μm. ot, optic tract; ac, anterior commissure; H, Hippocampus.

observed in LD, MD, or any of the anterior or midline nuclei (not shown).

Anterograde Label after Injections in Caudal STG: Hemisphere with MTL Lesion

Aspiration of MTL did not interrupt either of the above pathways exiting the caudal STG, and so the pattern of prefrontal terminal label in the lesioned hemisphere did not differ from that in the normal hemisphere.

Discussion

Before reviewing the anatomical findings, it is important to consider whether any of the results we have described could have arisen artifactually. For example, although we used a tracer, BDA 10K, that transports preferentially in the anterograde direction (Veenman et al. 1992; Reiner et al. 2000) and is therefore commonly used for this purpose, there may have been a small amount of bidirectional transport, and this could have resulted in labeling terminals belonging to axon

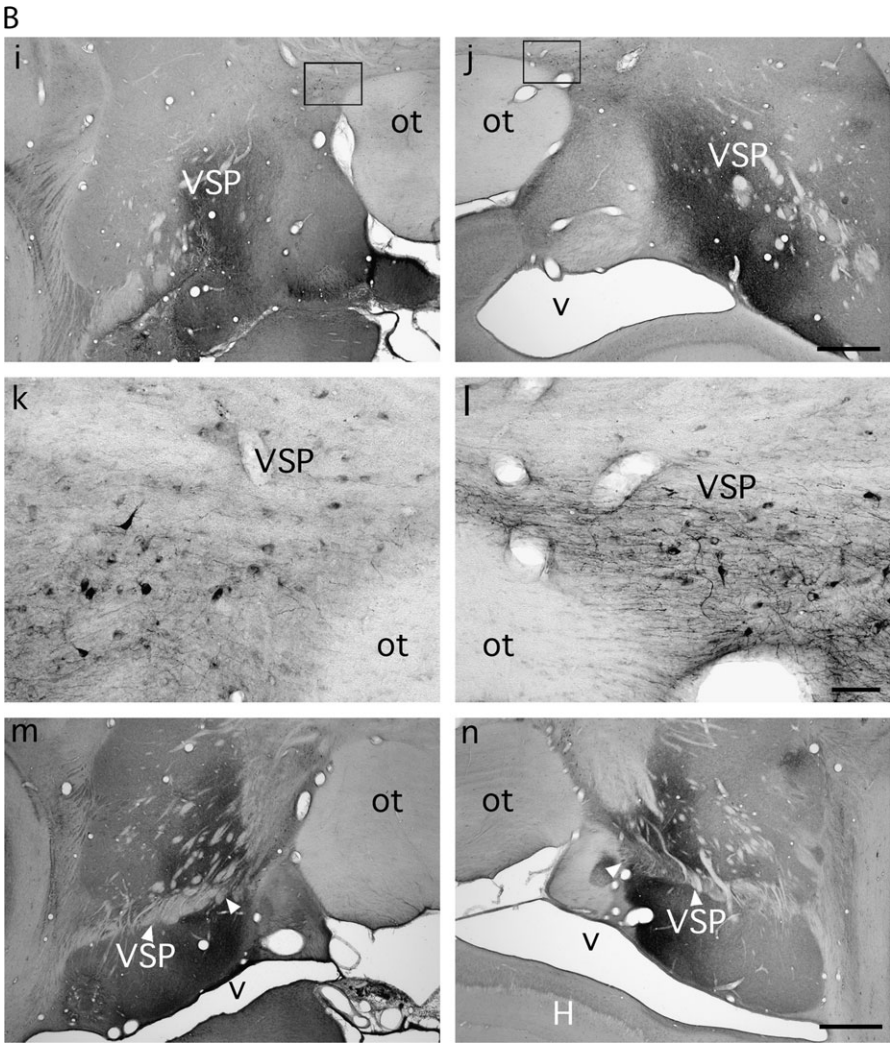

Figure 6. (Continued).

collaterals of cells located outside rSTG. Given the large amount of tracer we used, this possibility cannot be dismissed; yet, except for a few patches of cells in the basal forebrain (see Fig. 6*b*), we rarely encountered cells showing retrograde uptake. Also, any spurious anterograde terminal label resulting from such retrograde uptake would be present in both the normal and lesioned hemispheres and so would tend to reduce rather than exaggerate the effect of the disconnection. Further, spurious label due to the multiple tracer injections must have been minimal because we observed no projections that had not been seen previously in at least one study using single injections of BDA or other anterograde tracers (Carmichael and Price 1995b; Seltzer and Pandya 1989a; Barbas et al. 1999; Hackett et al. 1999; Romanski, Bates, et al. 1999; Romanski, Tian, 1999; Kondo et al. 2003.).

Another potential source of artifact are differences in the amount, locus, or extent of anterograde tracer that was injected into the 2 hemispheres that were being compared. In fact, the large series of injections we placed in rSTG in multiple cases minimized any such differences; and, importantly, the disconnection results were the same in every interhemispheric comparison despite the minor interhemispheric differences in these injections. In sum, there is strong reason to believe that the anatomical results reviewed below are both reliable and valid.

By placing an unusually large number of anterograde tracer injections in rostral STG and, separately, in auditory belt/parabelt areas of caudal STG, we were able to visualize the full extent of the projection pathways emanating from these particular auditory areas in each hemisphere and so reveal any and all points where the MTL lesion might disrupt those pathways. Our results indicate that aspiration of the piriform cortex, amygdala, and pes hippocampus, all located in the rostral portion of the MTL, disconnects parts of the prefrontal cortex and thalamus from auditory input arising in rSTG but not from auditory input originating in more caudal portions of the gyrus. The fibers from rSTG that were transected by the piriform/amygdala/pes hippocampus resections included 1) the medial part of the UF, with concomitant loss of labeled terminals primarily in ventral medial frontal cortex and secondarily in orbital frontal cortex, and 2) the VAP and VSP, respectively, both accompanied by loss of labeled terminals in the medial thalamus (Fig. 9). Like the fibers from caudal STG, which travel to the frontal lobe through the more laterally located external and extreme capsules, fibers from rSTG that travel either through those capsules or through the lateral part

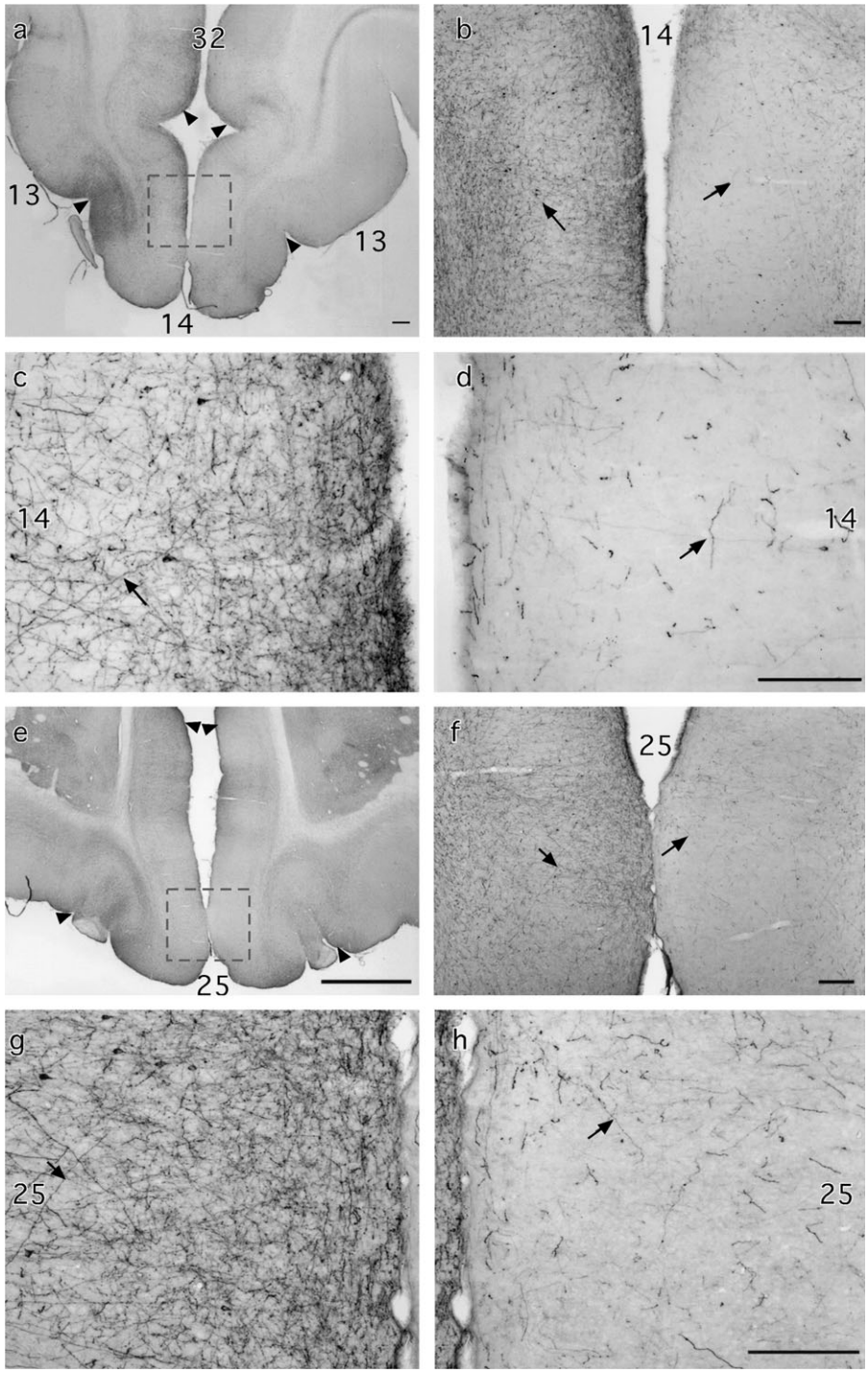

Figure 7. Photomicrographs of the ventral medial frontal cortex comparing the label after rSTG injections in the normal and MTL-lesioned hemispheres of Case M2. Area inside dashed-outline rectangles in (*a*) and (*e*) shown at higher magnification in (*b–d*) and (*f–h*), respectively. Arrows identify labeled axons in photomicrographs at low and high power magnifications. Scale bar: 250 μm.

of the UF, escaped damage. The spared lateral pathways terminate primarily in lateral frontal cortex, but also secondarily in orbital frontal areas, accounting for the relative sparing of terminals in orbital as compared with ventral medial frontal cortex. Also spared were fibers from STG projecting to the thalamus (e.g., pulvinar) via tracts outside the VAF and VAP, such as the temporal bundle of Arnold (Saunders et al. 2005). Before considering the behavioral implications of the anatomical disconnection results, it is important to compare the findings in the normal hemispheres with projection patterns that have already been described in the literature.

First, our results confirm that rSTG sends a major projection to ventral medial prefrontal cortical areas 14, 24, 25, and 32, with somewhat less dense projections to orbital frontal areas 12 and 13 (Petrides and Pandya 1988; Carmichael and Price 1995b; Barbas et al. 1999; Hackett et al. 1999; Romanski, Bates,

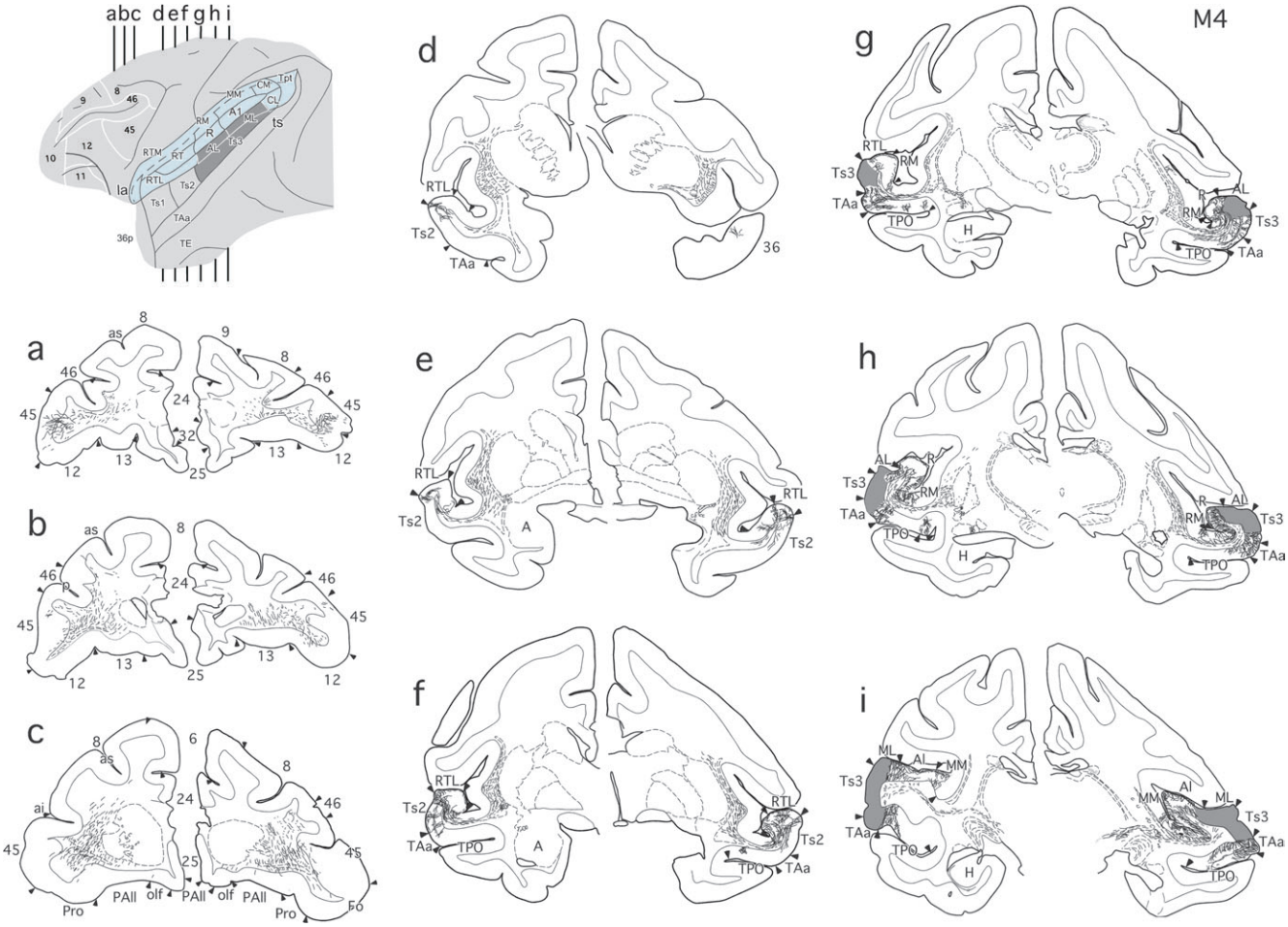

Figure 8. Lateral surface view and coronal sections (*a–i*) illustrating anterograde tracer injections in caudal STG (dark gray), with "opened" lateral sulcus shown in blue and resulting fiber and terminal label in case M4. Labeled fibers course through the white matter of the STG and the extreme and external capsules (*i–f*) rostrally and then just dorsal to the UF towards the frontal lobe. The pattern and density of label was the same in both hemispheres, suggesting that the MTL removal did not disrupt fibers from the caudal STG to the frontal lobe. A, amygdala; p, principal sulcus; see previous figures for abbreviations.

et al. 1999; Romanski, Tian, et al. 1999; Kondo et al. 2003, Saleem et al. 2008). We also confirm projections from the belt and parabelt regions to the lateral frontal areas 46, 45, and 12 (e.g., Hackett et al. 1999; Romanski et al. 1999a, 1999b; Saleem et al. 2008). The overall pattern is therefore consistent with the proposal that the caudal-rostral dimension in superior temporal cortex projects to the lateral-medial dimension in frontal cortex (Carmichael and Price 1995b; Pandya 1995; Barbas et al. 1999; Hackett et al. 1999; Romanski et al. 1999a, 1999b; Kondo et al. 2003). In the present study, the projections arising in caudal STG appeared less substantial than those originating from rostral STG, although this apparent difference in density

Figure 9. Summary diagrams of the major fiber pathways examined in this study. Left column of coronal sections illustrates projections from the rSTG to the frontal cortex and medial thalamus. The series of sections depicts each pathway's trajectory, from its origin in the injected cortical tissue (shown in black), to the course it follows through the white matter (black lines of varying thickness, representing graded size of projections), to its destination in cortex or thalamus (shown in shades of gray, representing graded density of terminal label). The projection from rSTG to the frontal cortex travels through the uncinate fasciculus (UF, +20). A major branch of this pathway continues medially to course below the striatum on the unoperated side (left hemisphere, solid line with arrowhead at +20) and then turns rostrally to terminate in medial and orbital frontal cortical areas on this side (left hemisphere, solid lines and dark gray shading at +24 and +30), with the highest density of terminal label in the ventral medial frontal cortical areas. Aspiration of the MTL (right MTL lesion at +7 through +20) transected this medial branch of the UF (right hemisphere, dashed line with arrowhead at +20) and, as a result, there was only sparse terminal label in the ventral medial frontal cortical areas on this side (right hemisphere, dashed lines with arrowheads and light gray shading at +24 and +30). Some fibers comprising the UF do not continue medially from their origin but, instead, turn dorsally and rostrally to travel through the external and extreme capsules (left hemisphere, solid lines at +15 and +20), after which they converge with the more medial branch of the uncinate fasciculis to terminate in mid and lateral orbital areas as well as in small frontal areas dorsally (left hemisphere, thin solid lines with arrowheads and light gray shading at +24 and +30). These branches of the UF escaped damage on the lesioned side and so the terminal label at their destinations was unaffected. The MTL removal also transected the caudally projecting fibers that join the VAP (at +15) and VSP (at +10 and +7), resulting in reduced terminal label in the medial thalamus (AN and MD at +10 and +7). Right column of coronal sections depicts projections to the frontal cortex from the injected areas of the auditory belt and parabelt divisions of the caudal STG. The MTL removal had no effect on these fiber pathways (solid black lines in all coronal sections, and so the terminal label was also unaffected (equivalent gray shading in both hemispheres at +24 and +30). AN, anterior thalamic nuclei; ai, arcuate sulcus, inferior; as, arcuate sulcus, superior; cc, corpus callosum; ci, cingulate sulcus; Cl, claustrum; lag, insula, agranular subdivision; ldg, insula, dysgranular subdivision; los, lateral orbital sulcus; orl, lateral orbital sulcus; orm, medial orbital sulcus; FO, frontal operculum; fx, fornix; Gp, globus pallidus; H, hippocampus; Pu, putamen; sf, subfascicular nucleus; MD, medial dorsal thalamic nucleus; see Figure 1 for abbreviations.

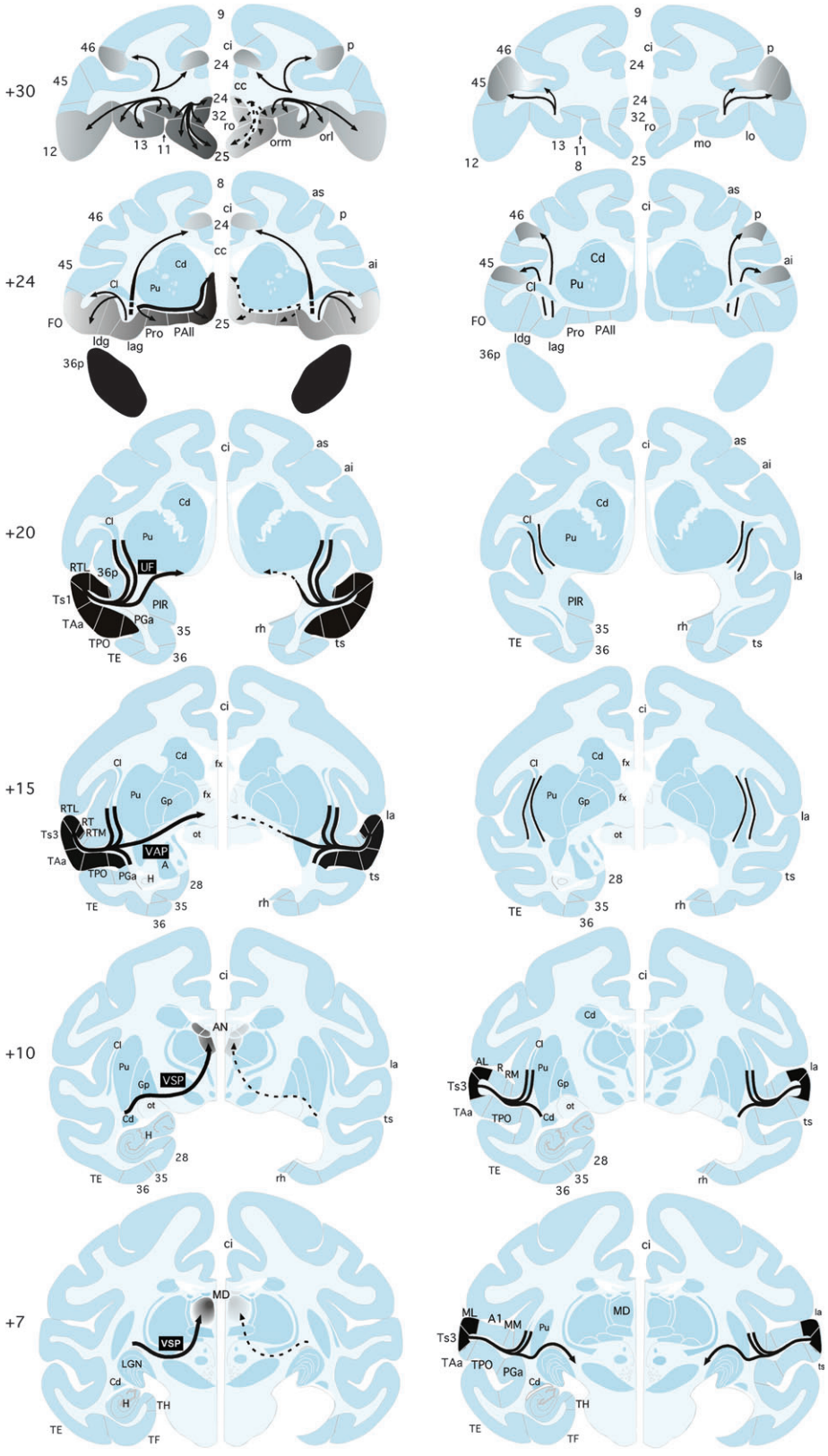
+30
+24
+20
+15
+10
+7
9
ci
p
46
45
24
cc
32
ro
12
13
11
25
orm
orl
8
as
ai
Cd
Cl
Pu
FO
Pro
PAll
ldg
lag
36p
UF
RTL
Ts1
PIR
PGa
TAa
TPO
TE
35
36
rh
ts
la
fx
Gp
RT
RTM
Ts3
ot
VAP
A
H
28
AN
VSP
LGN
MD
TH
TF
mo
lo
AL
R
RM
ML
A1
MM

could simply reflect the much larger number of injections placed in rSTG.

The experimental approach we used does not of course allow distinguishing among the projections arising from different divisions of rSTG. However, previous reports (Carmichael and Price 1995a, 1995b; Barbas et al. 1999; Hackett et al. 1999; Romanski, Bates, et al. 1999; Romanski, Tian, et al. 1999; Kondo et al. 2003) suggest that the superior temporal pole projects almost exclusively to the ventral medial frontal cortex (areas 14, 24, 25, 32), whereas the efferents from tissue behind the pole (e.g., Ts1 and Ts2) target not only the medial but also the orbital (areas 11, 12, and 13) and lateral (areas 12, 45, 46, and 9) prefrontal cortex (Carmichael and Price 1995b; Barbas et al. 1999; Hackett et al. 1999; Romanski, Bates, et al. 1999; Romanski, Tian, et al. 1999; Kondo et al. 2003). The present results, which include all these target areas, are therefore consistent with the proposed organization of the projections from the different subdivisions of rSTG. They do suggest, however, that the projection to orbital areas 11, 12, and 13 may be larger than previously reported (Carmichael and Price 1995b; Kondo et al. 2003; Saleem et al. 2008), a difference that may be due to our having placed tracers throughout rSTG rather than in selected subdivisions. Similarly, the projection to the thalamus arises primarily from area 36p of the temporal pole and much less so from more caudal areas (Russchen et al. 1987; Gower 1989).

Our results also clearly reveal the major efferent fiber routes leaving the STG, and the delineation of these pathways allowed us to identify the points where they were disrupted by the MTL lesion. The projections from rSTG to the ventral medial prefrontal cortex pass immediately lateral and dorsal to the piriform cortex/rostral amygdala and form the medial portion of the UF. It is just this medial portion that is disrupted by the rostral part of the MTL removal, leaving largely intact the lateral portion of the UF as well as fibers contributing to the external and extreme capsules. Therefore, medial frontal cortex had a reduced density of labeled fibers, whereas the density of label in lateral orbital and inferior prefrontal convexity remained relatively unchanged. This suggests a topographical organization in the arrangement of the superior temporal projection fibers that comprise the UF. Furthermore, the relative sparing of the external and extreme capsules may account for some of the sparing of the terminal label in the ventral medial and orbital frontal areas.

Removal of more caudal parts of the amygdala interrupted fibers from the rSTG that, like the fibers of the UF, also course just lateral and dorsal to this structure but then merge with the VAP, which turns caudally to reach the medial thalamus. The interruption of this fiber bundle led to a substantial decrease in the density of anterograde label in the anterior and midline nuclei and, particularly, in the MDmc.

Finally, the removal of the pes hippocampus included the most rostral portion of the roof of the temporal horn of the lateral ventricle, a white matter region containing rSTG fibers that merge with the VSP, which parallels the trajectory of the VAP to the thalamus. Severing these fibers therefore contributed to the medial thalamic disconnection.

Turning to the behavioral implications of the study, the results provide new support for the possibility described in detail at the outset that the impairment produced by MTL lesions on auditory DMS with short delays resulted from disconnection of rSTG from frontal cortex, medial thalamus, or both (Fritz et al. 2005). As indicated earlier, removal of rSTG and, separately, MTL resulted in deficits on auditory DMS that were independent of delay duration, appearing even at delays of less than 5 s, suggesting that each of these ablations impaired auditory short-term or working memory. Moreover, the same effect was not produced by removal of the hippocampal system alone, which, in any event, would ordinarily be expected to impair long-term, not short-term, memory. Interestingly, that negative finding is consistent with the results of the present study, which indicate that the part of the MTL removal that was primarily responsible for the disconnection was severance of white matter tracts accompanying aspiration of the amygdala, although transection of tracts attending aspiration of the pes hippocampus contributed to disconnection of the medial thalamus.

These considerations lead to the conclusion that, if the auditory memory impairment after MTL ablation is attributable to disconnection of downstream areas from rSTG, then the critical tissue must be located within either the ventral medial frontal cortex, or the medial thalamus, or both. The alternative possibility noted in the Introduction, that the critical area of deafferentation might be located instead in the lateral prefrontal cortex (i.e., lateral 12, 45, and 46) is ruled out by the finding that this area was not disconnected from its sources of auditory input in either rSTG or the more caudally situated belt and parabelt areas (Hackett et al. 1999; Romanski, Bates, et al. 1999; Romanski, Tian, et al. 1999).

Although the contributions of the ventral medial prefrontal cortex to auditory working memory is unknown, there is mounting evidence that this region plays an important role in processing species-specific vocalizations. Thus, electrical stimulation of medial prefrontal cortex elicits vocalizations (Robinson 1967), and electrophysiological studies (Vogt and Barbas 1988; Rolls et al. 2006) indicate that both this region and orbitofrontal cortex are responsive to conspecific calls, especially highly emotive ones. Further, a recent PET study in macaques (Gil-da-Costa et al. 2004) showed that area 32 is selectively activated by monkey screams as compared with coos and nonbiological sounds, and other neuroimaging findings (Poremba et al. 2004; Petkov et al. 2008) indicate that rSTG, the source of auditory input to medial and orbital frontal cortical areas, likewise contains tissue that is activated preferentially by conspecific calls.

As to the medial thalamus, nothing is currently known regarding its possible participation in either auditory working memory or auditory processing. Like the medial and orbital frontal cortical areas, however, with which it is reciprocally connected (Goldman-Rakic and Porrino 1985; Vogt and Barbas 1988; Bachevalier et al. 1997; Hsu and Price 2007), the medial thalamus forms part of the acoustically related cortico-thalamo-cortical loop that originates in rSTG. The functional interaction among these 3 areas is therefore likely to be close, and this together with the disconnection evidence opens up the possibility, which now needs to be tested, that all 3 areas could contribute to the monkey's auditory working memory ability.

Another, more certain, behavioral implication of the disconnection findings must also be noted, one that echoes a position advanced long ago by Horel (1978) but differing from that earlier proposal in the nature of the impairments that need to considered. As indicated at the outset, Murray and colleagues (Baxter et al. 1998; Goulet et al. 1998) had

previously reported that fibers from the rhinal cortical region to both the inferior prefrontal cortex and medial thalamus were severed by aspiration lesions of the amygdala. The present results expand these earlier findings and suggest that aspiration of the amygdala, together with that of the piriform cortex and pes hippocampus, disconnect the prefrontal cortex and thalamus not only from the visually dominant rhinal cortical areas but also from auditory areas in the rSTG. Interpretation of the behavioral effects of deep temporal-lobe ablation or pathology, whether in monkeys or in humans, must therefore take into account the possibility that functional impairments other than those now known to be attributable to damage of the MTL structures themselves, such as the deficit in long-term memory (cf. Horel 1978), might be due instead to transection of pathways connecting intact, rostral temporal neocortical areas with their targets in prefrontal and thalamic regions.

Funding

Funding for this article and for the Open Access publication charges for this article was provided by Intramural Research Program of the National Institute of Mental Health.

Notes

We wish to thank Helena Hernáez and Marta Fonollosa for their technical assistance and Tomas Cabárcos and Megan Malloy for their contributions to the preparation of the figures. *Conflict of Interest*: None declared.

Address correspondence to Monica Muñoz, Institute of Child Health, 30 Guilford Street, London WC1N 1EH, UK. Email: monica.munoz@ich.ucl.ac.uk.

References

Bachevalier J, Meunier M, Lu MX, Ungerleider LG. 1997. Thalamic and temporal cortex input to medial prefrontal cortex in rhesus monkeys. Exp Brain Res. 115:430–444.

Barbas H, Ghashghaei H, Dombrowski SM, Rempel-Clower NL. 1999. Medial prefrontal cortices are unified by common connections with superior temporal cortices and distinguished by input from memory-related areas in the rhesus monkey. J Comp Neurol. 410:343–367.

Barbas H, Pandya DN. 1989. Architecture and intrinsic connections of the prefrontal cortex in the rhesus monkey. J Comp Neurol. 286:353–375.

Baxter M, Saunders RC, Murray EA. 1998. Aspiration lesions of the amygdala interrupt connections between prefrontal cortex and the temporal cortex in rhesus monkeys. Soc Neurosci Abstr. 24:1905.

Buffalo EA, Ramus SJ, Clark RE, Teng E, Squire LR, Zola SM. 1999. Dissociation between the effects of damage to perirhinal cortex and area TE. Learn Mem. 6:572–599.

Carmichael ST, Price JL. 1994. Architectonic subdivision of the orbital and medial prefrontal cortex in the macaque monkey. J Comp Neurol. 346:366–402.

Carmichael ST, Price JL. 1995a. Limbic connections of the orbital and medial prefrontal cortex in macaque monkeys. J Comp Neurol. 363:615–641.

Carmichael ST, Price JL. 1995b. Sensory and premotor connections of the orbital and medial prefrontal cortex of macaque monkeys. J Comp Neurol. 363:642–664.

Fritz J, Mishkin M, Saunders RC. 2005. In search of an auditory engram. Proc Natl Acad Sci USA. 102:9359–9364.

Fuster JM, Alexander GE. 1971. Neuron activity related to short-term memory. Science. 173:652–654.

Gil-da-Costa R, Braun A, Lopes M, Hauser MD, Carson RE, Herscovitch P, Martin A. 2004. Toward an evolutionary perspective on conceptual representation: species-specific calls activate visual and affective processing systems in the macaque. Proc Natl Acad Sci USA. 101:17516–17521.

Goldman-Rakic PS. 1987. Circuitry of the prefrontal cortex and the regulation of behavior by representational knowledge. In: Mountcastle VB, Plum F, Geiger SR, editors. Handbook of physiology. Vol. 5. Bethesda (MD): American Physiological Society. p. 373–417.

Goldman-Rakic PS, Porrino LJ. 1985. The primate mediodorsal (MD) nucleus and its projection to the frontal lobe. J Comp Neurol. 242:535–560.

Goulet S, Dore FY, Murray EA. 1998. Aspiration lesions of the amygdala disrupt the rhinal corticothalamic projection system in rhesus monkeys. Exp Brain Res. 119:131–140.

Gower EC. 1989. Efferent projections from limbic cortex of the temporal pole to the magnocellular medial dorsal nucleus in the rhesus monkey. J Comp Neurol. 280:343–358.

Hackett TA, Stepniewska I, Kaas JH. 1999. Prefrontal connections of the parabelt auditory cortex in macaque monkeys. Brain Res. 817:45–58.

Horel JA. 1978. The neuroanatomy of amnesia: a critique of the hippocampal memory hypothesis. Brain. 101:403–445.

Hsu DT, Price JL. 2007. Midline and intralaminar thalamic connections with the orbital and medial prefrontal networks in macaque monkeys. J Comp Neurol. 504:89–111.

Insausti R, Amaral DG, Cowan WM. 1987. The entorhinal cortex of the monkey: II. Cortical afferents. J Comp Neurol. 264:356–395.

Iversen SD, Mishkin M. 1973. Comparison of the effects of superior temporal and inferior prefrontal lesions on auditory and non auditory tasks in rhesus monkeys. Brain Res. 55:355–367.

Kaas JH, Hackett TA. 2000. Subdivisions of auditory cortex and processing streams in primates. Proc Natl Acad Sci USA. 97:11793–11799.

Kondo H, Saleem KS, Price JL. 2003. Differential connections of the temporal pole with the orbital and medial prefrontal networks in macaque monkeys. J Comp Neurol. 465:499–523.

Lawicka W, Mishkin M, Rosvold HE. 1975. Dissociation of deficits on auditory tasks following partial prefrontal lesions in monkeys. Acta Neurobiol Exp. 35:581–607.

Malkova L, Bachevalier J, Mishkin M, Saunders RC. 2001. Neurotoxic lesions of perirhinal cortex impair visual recognition memory in rhesus monkeys. Neuroreport. 12:1913–1917.

Meunier M, Bachevalier J, Mishkin M, Murray EA. 1993. Effects on visual recognition of combined and separate ablations of the entorhinal and perirhinal cortex in rhesus monkeys. J Neurosci. 13:5418–5432.

Mishkin M. 1978. Memory in monkeys severely impaired by combined but not by separate removal of amygdala and hippocampus. Nature. 273:297–298.

Murray EA, Gaffan EA, Flint RW, Jr. 1996. Anterior rhinal cortex and amygdala: dissociation of their contributions to memory and food preference in rhesus monkeys. Behav Neurosci. 110:30–42.

Murray EA, Mishkin M. 1983. Severe tactual memory deficits in monkeys after combined removal of the amygdala and hippocampus. Brain Res. 270:340–344.

Murray EA, Mishkin M. 1984. Severe tactual as well as visual memory deficits follow combined removal of the amygdala and hippocampus in monkeys. J Neurosci. 4:2565–2580.

Olszewski J. 1952. The thalamus of the *Macaca mulatta*. An atlas for use with the stereotaxic instrument. Basel: Karger.

Pandya DN. 1995. Anatomy of the auditory cortex. Rev Neurol (Paris). 151:486–494.

Pandya DN, Rosene DL, Doolittle AM. 1994. Corticothalamic connections of auditory-related areas of the temporal lobe in the rhesus monkey. J Comp Neurol. 345:447–471.

Pandya DN, Sanides F. 1973. Architectonic parcellation of the temporal operculum in rhesus monkey and its projection pattern. Zeitschrift Anat Entwicklungsgesch. 139:127–161.

Pandya DN, Yeterian EH. 1990. Prefrontal cortex in relation to other cortical areas in rhesus monkey: architecture and connections. Prog Brain Res. 85:63–94.

Petkov CI, Kayser C, Steudel T, Whittingstall K, Augath M, Logothetis NK. 2008. A voice region in the monkey brain. Nat Neurosci. 11:367–374.

Petrides M, Pandya DN. 1988. Association fiber pathways to the frontal cortex from the superior temporal region in the rhesus monkey. J Comp Neurol. 273:52–66.
Petrides M, Pandya DN. 1999. Dorsolateral prefrontal cortex: comparative cytoarchitectonic analysis in the human and the macaque brain and corticocortical connection patterns. Eur J Neurosci. 11:1011–1036.
Petrides M, Pandya DN. 2002. Comparative cytoarchitectonic analysis of the human and the macaque ventrolateral prefrontal cortex and corticocortical connection patterns in the monkey. Eur J Neurosci. 16:291–310.
Poremba A, Malloy M, Saunders RC, Carson RE, Herscovitch P, Mishkin M. 2004. Species-specific calls evoke asymmetric activity in the monkey's temporal poles. Nature. 427:448–451.
Reiner A, Gamlin P. 1980. On noncarcinogenic chromogens for horseradish peroxidase histochemistry. J Histochem Cytochem. 28: 187–191.
Reiner A, Veenman CL, Medina L, Jiao Y, Del Mar N, Honig MG. 2000. Pathway tracing using biotinylated dextran amines. J Neurosci Methods. 103:23–37.
Robinson B. 1967. Vocalization evoked from forebrain in *Macaca mulatta*. Physiol Behav. 2:345–354.
Rolls ET, Critchley HD, Browning AS, Inoue K. 2006. Face-selective and auditory neurons in the primate orbitofrontal cortex. Exp Brain Res. 170:74–87.
Romanski LM, Bates JF, Goldman-Rakic PS. 1999. Auditory belt and parabelt projections to the prefrontal cortex in the rhesus monkey. J Comp Neurol. 403:141–157.
Romanski LM, Tian B, Fritz J, Mishkin M, Goldman-Rakic PS, Rauschecker JP. 1999. Dual streams of auditory afferents target multiple domains in the primate prefrontal cortex. Nat Neurosci. 2:1131–1136.
Rosene DL, Roy NJ, Davis BJ. 1986. A cryoprotection method that facilitates cutting frozen sections of whole monkey brains for histological and histochemical processing without freezing artifact. J Histochem Cytochem. 34:1301–1315.
Russchen FT, Amaral DG, Price JL. 1987. The afferent input to the magnocellular division of the mediodorsal thalamic nucleus in the monkey, *Macaca fascicularis*. J Comp Neurol. 256:175–210.
Saleem K, Kondo H, Price J. 2008. Complementary circuits connecting the orbital and medial prefrontal networks with the temporal, insular, and opercular cortex in the macaque monkey. J Comp Neurol. 506:659–693.
Saunders RC, Mishkin M, Aggleton JP. 2005. Projections from the entorhinal cortex, perirhinal cortex, presubiculum, and parasubiculum to the medial thalamus in macaque monkeys: identifying different pathways using disconnection techniques. Exp Brain Res. 167:1–16.
Seltzer B, Pandya DN. 1978. Afferent cortical connections and architectonics of the superior temporal sulcus and surrounding cortex in the rhesus monkey. Brain Res. 149:1–24.
Seltzer B, Pandya DN. 1989a. Frontal lobe connections of the superior temporal sulcus in the rhesus monkey. J Comp Neurol. 281:97–113.
Seltzer B, Pandya DN. 1989b. Intrinsic connections and architectonics of the superior temporal sulcus in the rhesus monkey. J Comp Neurol. 290:451–471.
Veenman CL, Reiner A, Honig MG. 1992. Biotinylated dextran amine as an anterograde tracer for single- and double-labeling studies. J Neurosci Methods. 41:239–254.
Vogt BA, Barbas H. 1988. Structure and connections of the cingulate vocalization region in the rhesus monkey. In: Newman JD, editor. The physiological control of mammalian vocalization. New York: Plenum Publ. Corp. p. 203–225.
Walker ER. 1940. A cytoarchitectural study of the prefrontal area of the macaque monkey. J Comp Neurol. 73:59–86.